Role of malectin in $Glc_2Man_9GlcNAc_2$-dependent quality control of α1-antitrypsin

Yang Chen[a], Dan Hu[a], Rikio Yabe[b], Hiroaki Tateno[b], Sheng-Ying Qin[a], Naoki Matsumoto[a], Jun Hirabayashi[b], and Kazuo Yamamoto[a]

[a]Department of Integrated Biosciences, Graduate School of Frontier Sciences, University of Tokyo, 277-8562 Chiba, Japan; [b]Research Center for Medical Glycoscience, Advanced Industrial Science and Technology, Ibaraki 305-8568, Japan

ABSTRACT **Malectin was first discovered as a novel endoplasmic reticulum (ER)–resident lectin from *Xenopus laevis* that exhibits structural similarity to bacterial glycosylhydrolases. Like other intracellular lectins involved in glycoprotein quality control, malectin is highly conserved in animals. Here results from in vitro membrane-based binding assays and frontal affinity chromatography confirm that human malectin binds specifically to $Glc_2Man_9GlcNAc_2$ (G2M9) N-glycan, with a K_a of 1.97×10^5 M^{-1}, whereas binding to $Glc_1Man_9GlcNAc_2$ (G1M9), $Glc_3Man_9GlcNAc_2$ (G3M9), and other N-glycans is barely detectable. Metabolic labeling and immunoprecipitation experiments demonstrate that before entering the calnexin cycle, the folding-defective human α1-antitrypsin variant null Hong Kong (AT^{NHK}) stably associates with malectin, whereas wild-type α1-antitrypsin (AT) or N-glycan–truncated variant of AT^{NHK} (AT^{NHK}-Q3) dose not. Moreover, malectin overexpression dramatically inhibits the secretion of AT^{NHK} through a mechanism that involves enhanced ER-associated protein degradation; by comparison, the secretion of AT and AT^{NHK}-Q3 is only slightly affected by malectin overexpression. ER-stress induced by tunicamycin results in significantly elevated mRNA transcription of malectin. These observations suggest a possible role of malectin in regulating newly synthesized glycoproteins via G2M9 recognition.**

Monitoring Editor
Reid Gilmore
University of Massachusetts

Received: Mar 9, 2011
Revised: Jul 15, 2011
Accepted: Jul 22, 2011

INTRODUCTION

The endoplasmic reticulum (ER) is a highly specialized compartment for the synthesis and maturation of proteins destined for secretion, the plasma membrane, or intracellular organelles. A variety of ER-resident lectins and molecular chaperones facilitate the correct folding and assembly of nascent N-glycosylated proteins (Helenius and Aebi, 2004; Lederkremer, 2009). N-glycosylation is initiated by oligosaccharyltransferase (OST), which catalyzes the transfer of $Glc_3Man_9GlcNAc_2$ (G3M9) from lipid-linked intermediates to target asparagine residues within the sequence Asn-X-Ser/Thr in newly synthesized peptides. The outermost two glucose residues of G3M9 glycan are trimmed by α-glucosidase I (GI) and II (GII), and then monoglucosylated $Glc_1Man_9GlcNAc_2$ (G1M9) is trapped by calnexin/calreticulin (CNX/CRT) through the N-glycan. Removal of the innermost glucose is catalyzed by GII, and then the glycoprotein is released from the CNX/CRT complex. The conformation of the released glycoprotein is validated by the folding sensor UDP-Glc:glycoprotein glucosyltransferase 1 (UGGT), which recognizes exposed hydrophobic patches on unfolded proteins (Taylor *et al.*, 2004; Totani *et al.*, 2009). Misfolded glycoproteins are reglucosylated by UGGT, again captured by CNX/CRT, and then processed by a CNX/CRT–associated protein–disulfide bond isomerase, ERp57, which restores their proper conformation (Zapun *et al.*, 1998). After several such cycles, the correctly folded glycoprotein escapes from the CNX/CRT complex and transits from the ER to the Golgi. Misfolded glycoproteins also exit the cycle but are targeted for ER-associated degradation (ERAD) with the aid of osteosarcoma 9 (OS-9) (Bernasconi *et al.*, 2008; Hosokawa *et al.*, 2009; Mikami *et al.*, 2010) and XTP3-B (Hosokawa *et al.*, 2008; Yamaguchi *et al.*, 2010).

This article was published online ahead of print in MBoC in Press (http://www.molbiolcell.org/cgi/doi/10.1091/mbc.E11-03-0201) on August 3, 2011.

Address correspondence to: Kazuo Yamamoto (yamamoto@k.u-tokyo.ac.jp).

Abbreviations used: AT, α1-antitrypsin; AT^{NHK}, α1-antitrypsin variant null(Hong Kong); CNX, calnexin; CST, castanospermine; DNJ, 1-deoxynojirimycin; endo H, endo-β-*N*-acetylglucosaminidase H; ER, endoplasmic reticulum; ERAD, endoplasmic reticulum–associated degradation; FAC, frontal affinity chromatography; Glc, glucose; GlcNAc, *N*-acetylglucosamine; KIF, kifunensine; Man, mannose; OS-9, osteosarcoma 9; PE, *R*-phycoerythrin; SA, streptavidin; SW, swainsonine.

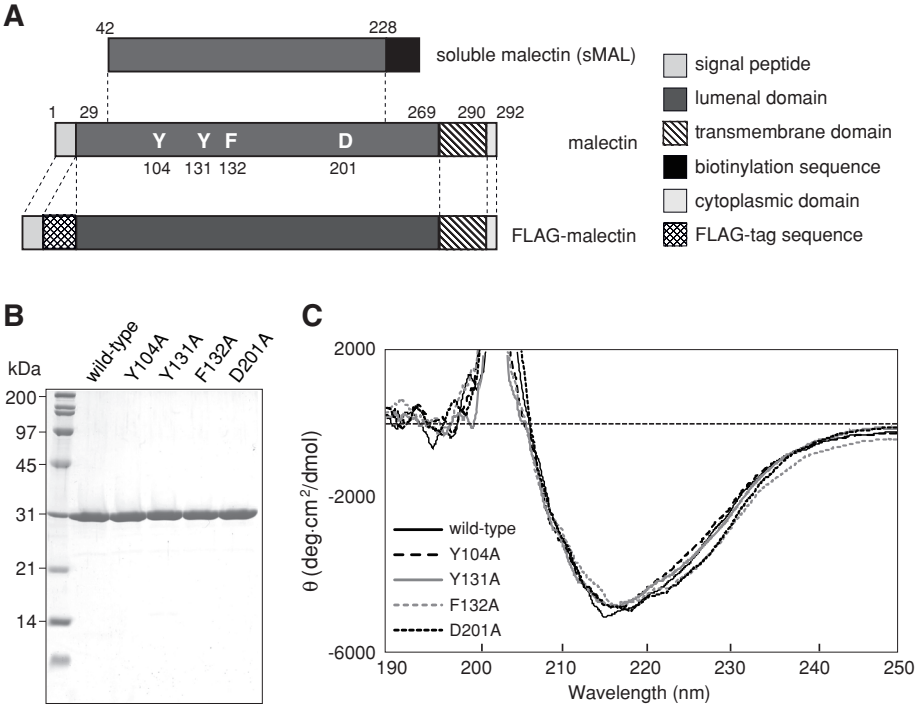

FIGURE 1: Purification of recombinant malectin and malectin mutants. (A) Construction of *E. coli* expression vectors for recombinant malectin and malectin mutants. (B) Recombinant malectin and malectin mutants were refolded from inclusion bodies and purified. The proteins were analyzed by SDS–PAGE and visualized with Coomassie brilliant blue. (C) CD spectra of wild-type and mutant malectins were obtained as described in *Materials and Methods*.

The trimming of two glucose residues from G3M9 allows the glycoprotein to enter the CNX/CRT cycle of protein folding. It is not clear why cells require both GI and GII trimming of G3M9 for recognition by CNX/CRT. Recently, a novel membrane-anchored ER lectin, termed malectin, was identified in *Xenopus laevis* and was found to be highly conserved in animals (Schallus *et al.*, 2008). Nuclear magnetic resonance (NMR) analysis revealed precise details of the interaction of the carbohydrate-binding domain of malectin and Glcα1,3Glc (Schallus *et al.*, 2010). It was subsequently shown using glycan analysis that *X. laevis* and human malectin selectively bind to Glcα1,3Glc, Glcα1, 4Glc, Glcβ1,6Glc, and $Glc_2Man_7GlcNAc_1$ (G2M7GN1; Palma *et al.*, 2010). However, the role of malectin and the first glucose-trimming process remains to be elucidated.

Human α1-antitrypsin (AT) is a glycoprotein with three N-glycan moieties attached to the peptide chain. It is synthesized as a soluble form in the ER, acquires complex-type glycans in the Golgi, and is ultimately secreted into the blood, where it functions to prevent the proteolytic degradation of lung elastin (Travis and Salvesen, 1983). It has been reported that interactions between several ER-resident lectins and the N-glycans on AT assist in the correct folding and secretion of AT (Ou *et al.*, 1993; Nyfeler *et al.*, 2008). A carboxyl terminus–truncated AT variant termed null(Hong Kong) (AT^{NHK}; Sifers *et al.*, 1988) exhibits a defective folding phenotype and has been used as a tool for studies of ERAD (Liu *et al.*, 1999; Hosokawa *et al.*, 2001). Terminally misfolded proteins tend to display hydrophobic patches on their surface, which causes aggregation. Molecular chaperones in the ER prevent this aggregation by capturing misfolded proteins (Hartl, 1996; Bukau *et al.*, 2000). Le *et al.* (1994) showed that CNX selectively bound to AT^{NHK}, which indicates that CNX may be involved in monitoring the folded state of glycoproteins. Given the critical role of G1M9 glycan in the correct folding of glycoproteins in the CNX/CRT cycle, we asked whether malectin, which can recognize $Glc_2Man_9GlcNAc_2$ (G2M9) glycan, plays a similar role in glycoprotein folding.

The present study demonstrated that human malectin specifically recognizes G2M9 with a K_a of 1.97×10^5 M^{-1}, based on the use of a membrane-based binding assay (Yamamoto and Kawasaki, 2010) and frontal affinity chromatography (FAC; Tateno *et al.*, 2007). In cells, human malectin stably interacted with newly synthesized AT^{NHK}, but not AT, via G2M9 glycans. The interaction of AT^{NHK} with malectin resulted in enhanced ERAD of AT^{NHK} and prevented the secretion of the misfolded glycoprotein. These findings provide evidence of a possible role of malectin in N-glycosylated protein quality control via recognition of G2M9.

RESULTS

Human malectin binds to HeLaS3 cells treated with 1-deoxynojirimycin

The recently identified ER-resident membrane protein malectin selectively binds to nigerose (Glcα1,3Glc) and $Glc_2Man_7GlcNAc_1$ (G2M7GN1) in *X. laevis,* suggesting that it might bind to G2M9 glycan in the ER (Schallus *et al.*, 2008). Malectin is highly conserved across species, including humans. To investigate the possible role of malectin in glycoprotein quality control in the ER, we first examined the sugar-binding activity and specificity of human malectin to determine whether it was similar to that of *X. laevis* malectin.

The luminal region of malectin, termed sMAL, containing a C-terminal biotinylation site-tag (Figure 1A) was expressed in *Escherichia coli*, refolded, and purified by ion-exchange and gel filtration chromatography as a single 31-kDa band on SDS–PAGE (Figure 1B). After biotinylation with the biotin ligase BirA, purified biotinylated sMAL was incubated with *R*-phycoerythrin (PE)–labeled streptavidin (PE-SA) to form a PE-labeled sMAL tetramer (sMAL-SA) with increased sugar-binding avidity (Kawasaki *et al.*, 2007). The binding of sMAL to cell surface glycans was analyzed by flow cytometry using PE-labeled sMAL-SA. To generate cells that displayed different glycan patterns on their surface, HeLaS3 cells were treated with the α-glucosidase inhibitor castanospermine (CST) or 1-deoxynojirimycin (DNJ) or the α-mannosidase inhibitor kifunensine (KIF) or swainsonine (SW). CST preferentially inhibits the activity of α1,2-specific glucosidase I (GI; Figure 3A), and CST treatment of cells results in the accumulation of triglucosylated high mannose–type N-glycans (Sasak *et al.*, 1985). DNJ—the GI and α1,3-specific glucosidase II (GII) inhibitor—preferentially inhibited the activity of GII when a low concentration (2 μM) of DNJ was used in in vitro assay (Saunier *et al.*, 1982). To confirm this selective inhibitory effect of DNJ in cells, we compared the mobility of intracellular AT^{NHK} on SDS-polyacrylamide gel produced in the presence of CST, DNJ, or deoxymannojirimycin (DMJ, an ER α1,2-mannosidase I inhibitor). AT^{NHK} from 1 mM DNJ–treated HeLa cells migrated in the middle of AT^{NHK} from CST- and DMJ-treated cells. Furthermore, AT^{NHK} from 1 mM DNJ–treated cells was partially unsusceptible to Jack bean α-mannosidase (Supplemental Figure S1). These results indicated that 1 mM of DNJ preferentially inhibited GII and caused accumulation of G2M9 and/or $Glc_1Man_9GlcNAc_2$ (G1M9) in HeLa cells. KIF inhibits ER α1,

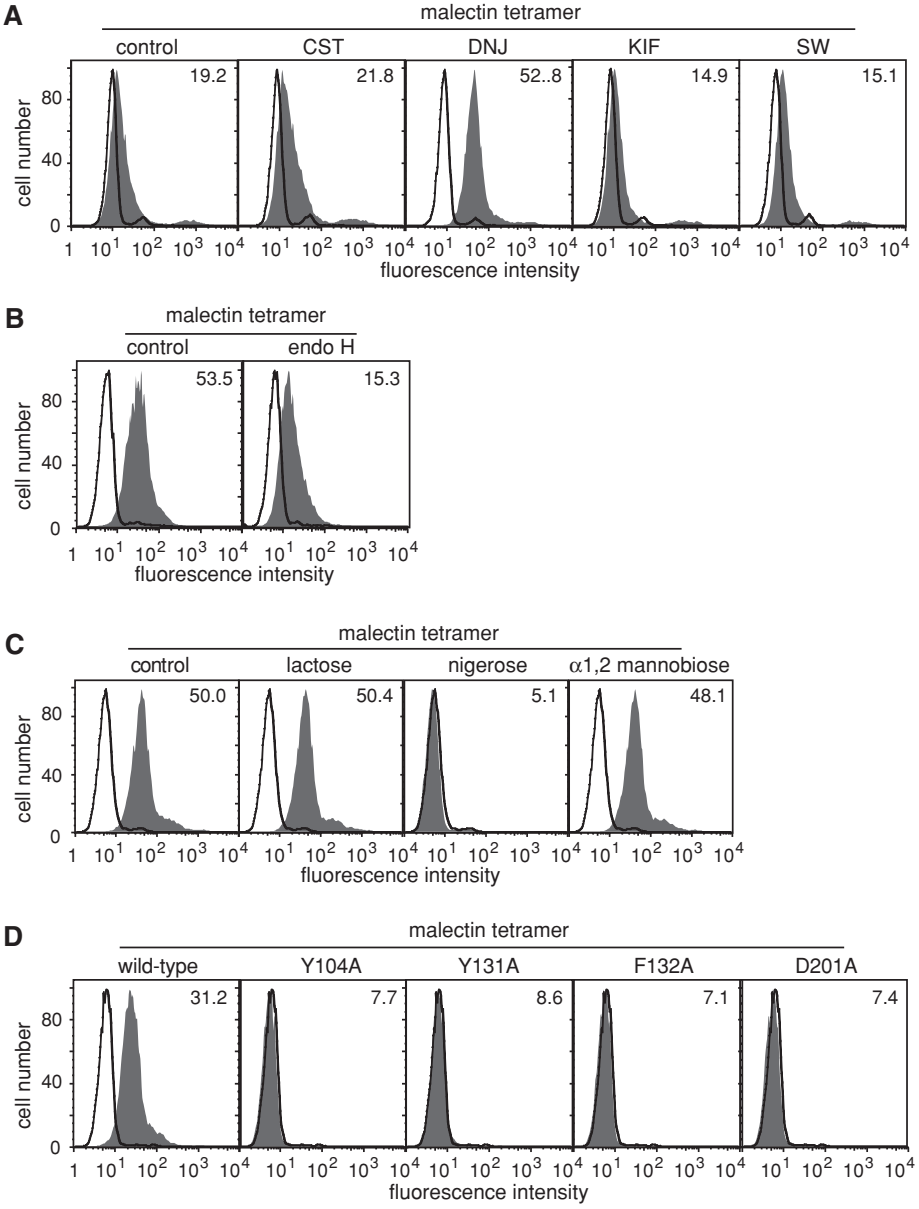

FIGURE 2: Malectin binds to N-glycans on the surface of DNJ-treated cells. (A) HeLaS3 cells treated with 1 mM CST, 1 mM DNJ, 8.6 μM KIF, or 58 μM SW for 20 h were incubated with 0.5 μg/ml PE-labeled sMAL-SA (filled histogram) or PE-SA as a control (thin line) and then analyzed by flow cytometry. (B) HeLaS3 cells cultured in the presence of 1 mM DNJ for 20 h were treated with or without 10^4 U/ml endo H and then incubated with PE-labeled sMAL-SA (filled histogram) or PE-SA as a control (thin line), followed by flow cytometry. (C) DNJ-treated HeLaS3 cells were incubated with 0.5 μg/ml PE-labeled sMAL-SA in the presence of 10 mM lactose, nigerose, or α1,2-mannobiose and then analyzed by flow cytometry. (D) DNJ-treated HeLaS3 cells were incubated with 0.5 μg/ml PE-labeled sMAL-SA or the indicated malectin mutant and then analyzed by flow cytometry. The numbers indicate the mean fluorescence intensity.

2-mannosidase I (Elbein *et al.*, 1990) and elicits expression of $Man_{8\text{-}9}GlcNAc_2$ glycans (M8, M9) on HeLaS3 cells (Kawasaki *et al.*, 2007). SW inhibits Golgi α-mannosidase II and blocks the processing of N-glycans from $GlcNAc_1Man_5GlcNAc_2$ to complex-type glycans (Tulsiani *et al.*, 1982, 1990). As shown in Figure 2A, PE-labeled sMAL-SA selectively bound to DNJ-treated HeLaS3 cells but not to CST-, KIF-, or SW-treated cells. These results indicate that human malectin binds to diglucosylated N-glycans on surfaces of cells. To confirm that the binding of malectin to DNJ-treated cells was through cell surface glycans, DNJ-treated HeLaS3 cells were treated with endo β-*N*-acetylglucosaminidase H (endo H), which cleaves high mannose–type glycans (Maley *et al.*, 1989). Endo H treatment significantly decreased the binding of sMAL-SA to DNJ-treated cells (Figure 2B), confirming that the binding of malectin to DNJ-treated HeLaS3 cells is through high mannose–type glycans. sMAL-SA was unable to bind KIF- and SW-treated cells, which suggests that terminal mannose residues are not sufficient for the binding of malectin and that Glcα1,3Glc of diglucosylated N-glycans is likely to be a major determinant for the binding of human malectin, as reported previously (Schallus *et al.*, 2008, 2010; Palma *et al.*, 2010).

To examine the requirement for Glcα1,3Glc structure in the binding of human malectin, a series of disaccharides was tested for their ability to inhibit binding of sMAL-SA to DNJ-treated cells (Figure 2C). The results showed that 10 mM nigerose (Glcα1,3Glc), but not lactose (Galβ1,4Glc) or α1,2-mannobiose (Manα1,2Man), decreased the binding of sMAL-SA to DNJ-treated cells. None of the monosaccharides tested abrogated binding, even at concentrations of 100 mM (unpublished data). These data suggested that the binding of malectin to DNJ-treated cells is mediated through the Glcα1,3Glc structure on diglucosylated N-glycans.

Human malectin selectively binds to G2M9

The sugar-binding specificity of human malectin was analyzed in more detail by FAC using a series of high mannose–type glycans (Figure 3B). Glucosylated high mannose–type glycans were also tested, including PA-labeled G3M9, G2M9, and G1M9. Of all the oligosaccharides tested, G2M9 was the only oligosaccharide recognized by malectin. The K_a for the interaction between malectin and G2M9 was $1.97 \times 10^5\ M^{-1}$ (Figure 3C). Although G1M9, G3M9, and M9 are structurally quite similar to G2M9, they were unable to bind to malectin. These results provided additional evidence that terminal Glcα1,3Glc moieties are the major determinant for the binding of malectin.

Mutation of conserved residues of malectin abrogates sugar binding

NMR analysis of the interaction between *X. laevis* malectin and Glcα1,3Glc demonstrated that five amino acid residues are involved in malectin binding to the disaccharide (Schallus *et al.*, 2008). These five residues are conserved in human malectin, corresponding to Tyr-82, Tyr-104, Tyr-131, Phe-132, and Asp-201. To determine whether any or all of these residues of human malectin were involved in binding to G2M9 glycan, we generated four single–amino acid substitution mutants, Y104A, Y131A, F132A, and D201A

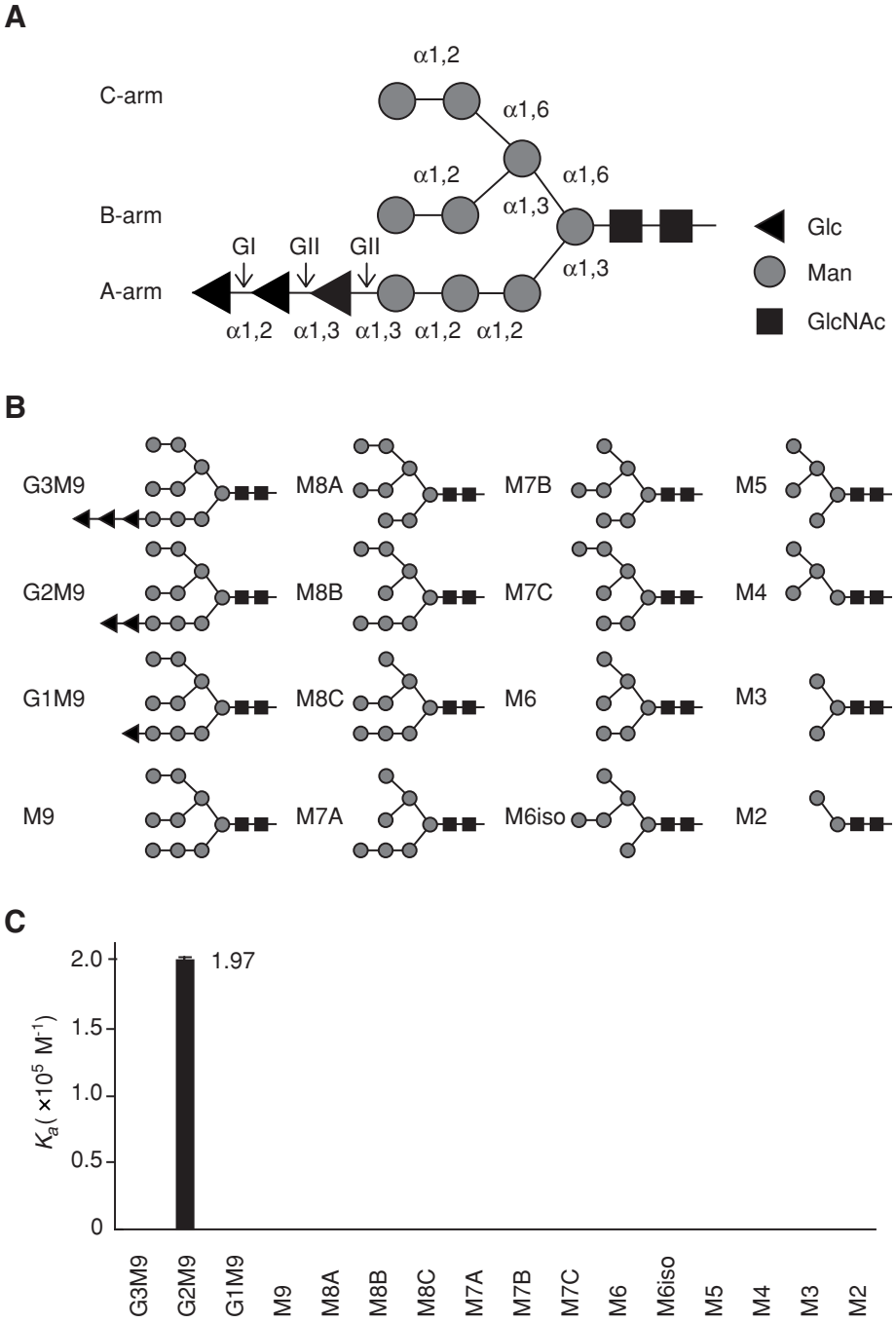

FIGURE 3: Malectin specifically binds to diglucosylated high mannose–type glycans. (A) Structure of the N-glycan precursor G3M9. The mannose residues are organized into three branches, with a triglucosylated A-arm and the 6′-pentamannosyl branch subdivided into B- and C-arms. GI hydrolyzes α1,2-linked glucose and GII cleavages α1,3-linked glucoses at two sites. (B) Structures of the PA-labeled N-glycans used for FAC. (C) The affinity of each PA-labeled oligosaccharide for human malectin was determined by FAC. The K_a values represent the results of three independent experiments.

(Figure 1, A and B) and examined their sugar-binding activity by flow cytometry. None of the mutations markedly affected protein folding, as the circular dichroism (CD) spectrum of each mutant protein was similar to that of wild-type malectin (Figure 1C). However, the mutations abolished binding of malectin to DNJ-treated HeLaS3 cells (Figure 2D). These results indicated that the binding of human malectin to G2M9 N-glycan is mediated by specific conserved amino acid residues.

Stable binding of malectin to AT^{NHK} in an N-glycan–dependent manner

The results of flow cytometry and FAC demonstrated that human malectin specifically binds to G2M9 glycan. To understand the biological role of malectin in the ER, we investigated whether malectin was involved in the folding or ERAD of glycoproteins. The misfolding of the human α1-antitrypsin variant AT^{NHK} is well characterized, and AT^{NHK} is a good substrate for ERAD (Liu *et al.*, 1999). Both wild-type AT (394 amino acids) and AT^{NHK} (333 amino acids) have three N-linked sugar chains attached to the peptide backbone. We generated a variant of AT^{NHK}, AT^{NHK}-Q3, in which the three N-glycosylation–site Asn residues were substituted with Gln as an approach to evaluating whether protein folding or ERAD depended on the presence of N-glycans. AT, AT^{NHK}, or AT^{NHK}-Q3 was expressed in HeLa cells along with FLAG-tagged malectin. Newly synthesized glycoproteins were metabolically labeled with ^{35}S-methionine and ^{35}S-cysteine for 3 h, and the expression of AT, AT^{NHK}, and AT^{NHK}-Q3 was confirmed by immunoprecipitation using an anti-AT antibody followed by autoradiography. The three proteins were easily distinguishable by their molecular weights (Figure 4A). AT^{NHK} and AT^{NHK}-Q3 formed partial dimers on SDS-polyacrylamide gels under nonreducing conditions (Figure 4A, asterisks), most likely due to interdisulfide bonding as a result of their misfolded conformation (Hosokawa *et al.*, 2006). AT^{NHK} dimers interacted weakly with FLAG-tagged malectin in coimmunoprecipitation experiments (Figure 4B, lane 3). The presence of AT^{NHK} in the precipitates was confirmed by immunoblot analysis using an anti-AT antibody (unpublished data). However, if N-glycan processing is very rapid and G1M9 and M9, but not G2M9, are the major N-glycans on AT^{NHK} (Hosokawa *et al.*, 2003), we would not be able to readily monitor newly synthesized AT, AT^{NHK}, or AT^{NHK}-Q3 associated with FLAG-tagged malectin. So the same experiment was performed in the presence of 1 mM DNJ to accumulate the G2M9 N-glycans. When lysates of DNJ-treated cells were subjected to immunoprecipitation using an anti-FLAG antibody, the amount of AT^{NHK} (dimers and monomers) that coprecipitated with malectin was markedly increased, and AT weakly coprecipitated (Figure 4B, lanes 5–8). The band corresponding to AT^{NHK}-Q3 was not detected in anti–FLAG-malectin precipitates. These results indicated that malectin selectively interacts with misfolded AT^{NHK}, and the interaction is N-glycan dependent. We next performed a pulse-chase experiment in which cells were pulse labeled with ^{35}S-Met and ^{35}S-Cys for 30 min, and then coprecipitation of AT and AT^{NHK} with malectin was monitored over a 240-min chase period in the absence of DNJ (Supplemental

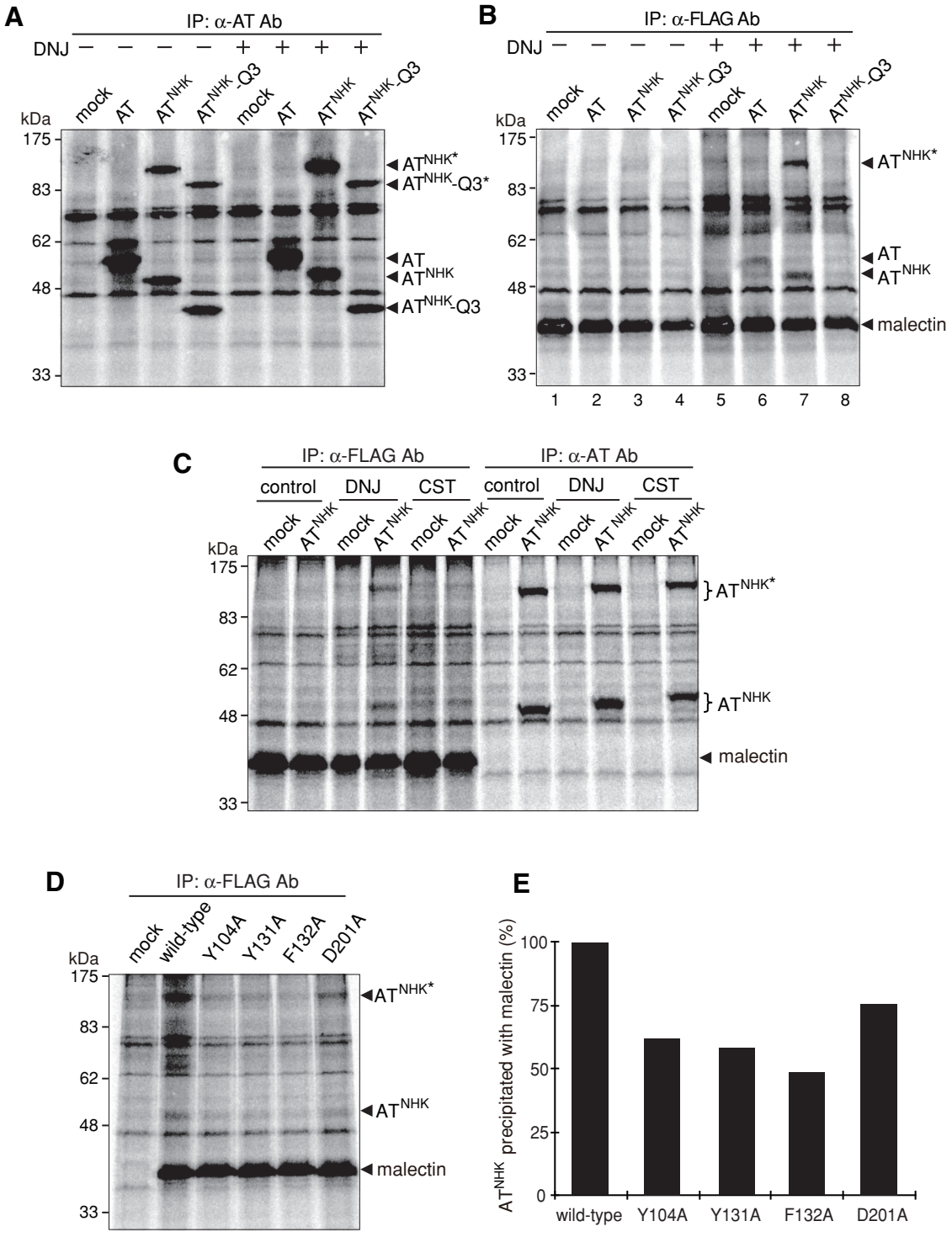

FIGURE 4: Significant interaction between malectin and AT^{NHK}. (A) HeLa cells were transfected with expression vectors for human AT, AT^{NHK} , and the N-glycosylation-deficient variant of AT^{NHK}, AT^{NHK}-Q3, along with FLAG-tagged malectin for 24 h. Cells were starved and then metabolically labeled with ^{35}S-methionine and ^{35}S-cysteine for 3 h. For DNJ treatment, the cells were cultured in the presence of 1 mM DNJ during the starvation and radiolabeling procedures. Cell lysates were subjected to immunoprecipitation using anti–human AT antibody (A) or anti-FLAG antibody (B), and then immune complexes were separated by SDS–PAGE under nonreducing conditions. Asterisk represents dimeric form. (C) HeLa cells were transfected with expression vectors for AT^{NHK} and FLAG-tagged malectin, radiolabeled, and then treated with 1 mM DNJ or CST. Radiolabeled cell lysates were subjected to immunoprecipitation using anti-FLAG antibody or anti–human AT antibody, and then immune complexes were analyzed by SDS–PAGE under nonreducing conditions. (D) HeLa cells were transfected with expression vectors for FLAG-tagged wild-type malectin or the indicated malectin mutants (Y104A, Y131A, F132A, or D201A) along with an expression vector for AT^{NHK}. Cells were radiolabeled and cultured in the presence of 1 mM DNJ. Radiolabeled cell lysates were subjected to immunoprecipitation using an anti-FLAG antibody; immune complexes were analyzed by SDS–PAGE under nonreducing conditions. (E) Quantification of the results in D.

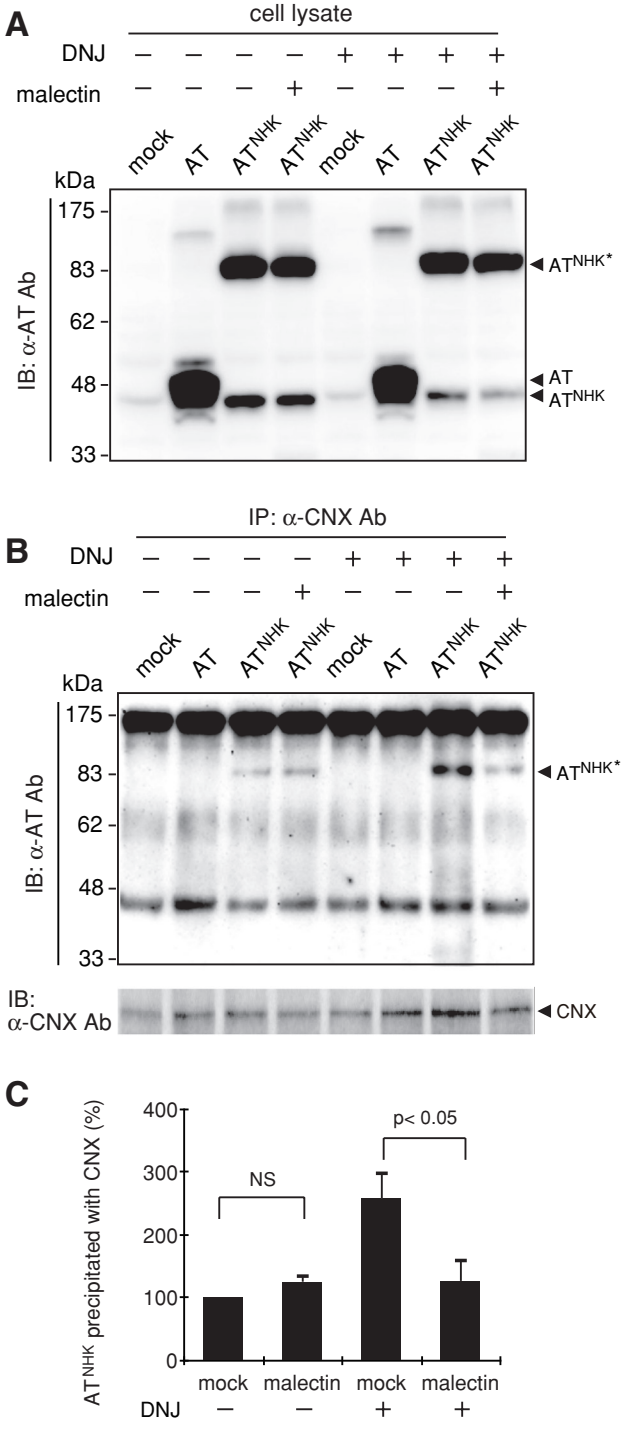

FIGURE 5: Overexpression of malectin reduces the association of CNX with AT^{NHK}. HeLa cells were cotransfected with pcDNA3.1-AT or pcDNA3.1-AT^{NHK} along with p3xFLAG-CMV9-malectin or an empty vector as a control. Cells were cultured in the presence or absence of 1 mM DNJ. Cell lysates were subjected to immunoprecipitation using anti-CNX antibody, and cell lysates (A) and immune complexes (B) were analyzed by SDS–PAGE under nonreducing conditions, followed by immunoblot using anti–human AT antibody. (C) Data of B were quantified by scanning densitometry. The data shown are mean ± SD from four independent experiments. NS, not significant.

Figure S2). There was evidence of a weak interaction between AT^{NHK} and malectin up to 120 min. By contrast, AT coprecipitated with malectin was barely detectable over the entire chase period. These results indicated that malectin stably binds to misfolded AT^{NHK} but not native AT. When the cells were treated with CST, coprecipitation of AT^{NHK} with malectin was decreased compared with DNJ-treated cells (Figure 4C). Furthermore, compared with wild-type malectin, coprecipitation of the sugar-binding-deficient mutants Y104A, Y131A, F132A, and D201A was decreased (Figure 4, D and E), despite being expressed at similar levels in HeLa cells. Moreover, double point mutants (Y104A/Y131A, Y104A/F132A, Y104A/D201A, or Y131A/F132A) bound to AT^{NHK} to a lesser extent than a single point mutant (Supplemental Figure S5, A and B). These results suggest that malectin interacts with AT^{NHK} in a G2M9 glycan–dependent manner.

Misfolded AT^{NHK} binds to malectin before entering the CNX cycle

CNX is a resident ER lectin specific for G1M9 N-glycan that functions as a chaperone, facilitating the folding of newly synthesized glycoproteins (Ware *et al.*, 1995). ERp57, which forms a complex with CNX, ensures the correct folding of unfolded and misfolded glycoproteins by catalyzing the oxidation–reduction of disulfide bonds (Zapun *et al.*, 1998). Similar to malectin, CNX also preferentially interacted with AT^{NHK} compared with wild-type AT (Figure 5B), regardless of the similar intracellular expression of the AT and AT^{NHK} (Figure 5A). CNX, however, specifically interacts with G1M9 glycan, whereas malectin preferentially binds to G2M9. To investigate whether malectin was involved in regulating the folding of AT^{NHK} upstream of CNX, we examined the effect of malectin overexpression on CNX binding to AT^{NHK}. AT^{NHK} and FLAG-tagged malectin were expressed in HeLa cells in the presence of 1 mM DNJ, which prolongs the processing of N-glycans and significantly enhances the trapping of AT^{NHK} by malectin (Figure 4B). Cell lysates were subjected to immunoprecipitation using an anti–human CNX antibody, and the amount of AT^{NHK} that coprecipitated with endogenous CNX was examined by immunoblotting using anti-AT antibody. In the presence of DNJ, interaction of AT^{NHK} with CNX was increased (Figure 5B). This showed that inhibition of glucose trimming from G1M9 glycan by DNJ enhanced this interaction (Hammond *et al.*, 1994). Overexpression of malectin in the presence of DNJ resulted in a decrease in the amount of AT^{NHK} that coprecipitated with CNX (Figure 5B). However, this decrease was canceled in the absence of DNJ (Figure 5B). In contrast, decreased expression of malectin by small interfering RNA elevated the interaction between AT^{NHK} and CNX (Supplemental Figure S4). These results indicated that malectin down-regulates free AT^{NHK} upstream of CNX, consistent with the sugar-binding specificities of malectin and CNX.

Malectin overexpression abrogates the secretion of AT^{NHK}

The secretion and intracellular levels of AT, AT^{NHK}, and AT^{NHK}-Q3 were examined in cells that overexpressed malectin. Twenty-four hours after transfection, cells were starved for 48 h in serum-free medium, after which the culture supernatants and cells were collected. The level of AT, AT^{NHK}, and AT^{NHK}-Q3 in the culture medium and in cell lysates was monitored by immunoblot using an anti-AT antibody. Equal loading of proteins was confirmed by immunoblot analysis of β-actin and FLAG-tagged malectin in each sample (Figure 6A). Under such conditions, the levels of wild-type AT were higher in the culture medium than in cell lysates, which indicated that AT was actively secreted from the cell (Figure 6B). By contrast, AT^{NHK} and N-glycan–deficient AT^{NHK}-Q3 were present predominantly in the intracellular fraction (Figure 6C), most likely due to retention in the cell through interactions with chaperones or elimination through ERAD (Liu *et al.*, 1999). There was a low level of

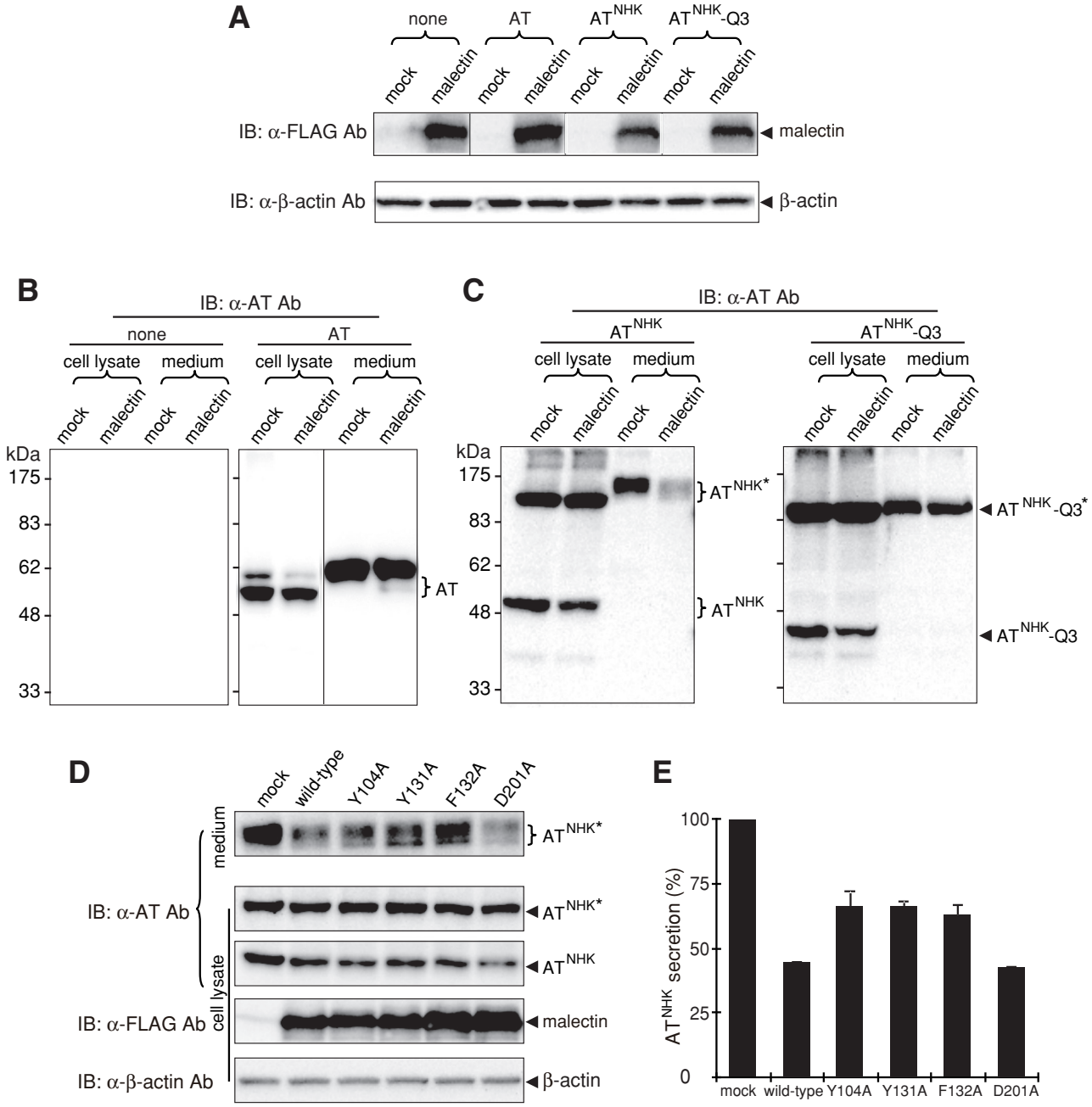

FIGURE 6: Malectin overexpression abrogates the secretion of AT^{NHK}. HeLa cells were transfected with expression vectors for FLAG-tagged malectin and AT, AT^{NHK}, or AT^{NHK}-Q3 for 24 h. Cells were cultured in serum-free medium for 48 h, and then cell lysate and medium were collected. (A) To confirm the expression levels of FLAG-tagged malectin, immunoblot was performed using anti-FLAG and anti–β-actin antibodies, respectively. The presence of AT (B) AT^{NHK} and AT^{NHK}-Q3 (C) in the cell lysate or culture medium was analyzed by immunoblot using an anti–human AT antibody. (D) HeLa cells were transfected with expression vectors for FLAG-tagged malectin or the indicated malectin mutants along with AT^{NHK}. Secreted and intracellular AT^{NHK}, FLAG-tagged malectin, and β-actin were analyzed by immunoblot. (E) Data were quantified by scanning densitometry from fluorographs. Secreted AT^{NHK} in the culture medium was detected by immunoblot using an anti–human AT antibody. Data are representative of two independent experiments.

secretion, however, which was consistent with previous reports (Bernasconi *et al.*, 2008). AT^{NHK} and AT^{NHK}-Q3 were secreted primarily as dimers, whereas secreted AT was monomeric. This could be due to the presence of interdisulfide bond(s) in misfolded AT^{NHK} and AT^{NHK}-Q3 (Hosokawa *et al.*, 2006). The amounts of secreted and intracellular wild-type AT were similar in the presence or absence of malectin overexpression (Figure 6B). By contrast, the amount of secreted AT^{NHK} was markedly decreased in malectin-overexpressing cells compared with mock-transfected cells, although the levels of intracellular AT^{NHK} were similar (Figure 6C, left). Decreased secretion of AT^{NHK} by overexpression of malectin was also reported by Galli *et al.* (2011). Of interest, deletion of the N-glycan moieties from AT^{NHK} abrogated this decrease in secretion by malectin overexpression (Figure 6C, right). Furthermore, decreased secretion of AT^{NHK} induced by malectin overexpression was less effective when the sugar-binding–deficient malectin with a

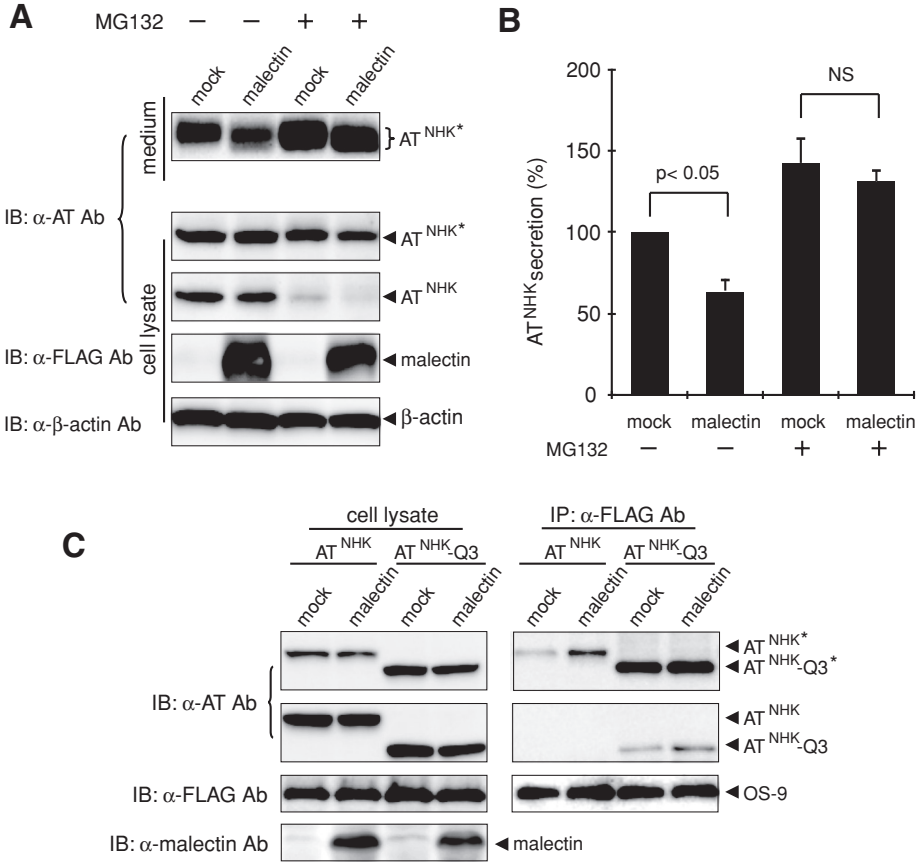

FIGURE 7: Downregulation of AT^{NHK} secretion is due to enhancement of ERAD. (A) HeLa cells were transfected with expression vectors for FLAG-tagged malectin, or empty vector, and AT^{NHK}. After 24 h, cells were cultured in complete medium containing 2 μM MG132. The culture medium and cell lysates were collected 48 h later. Secreted and intracellular AT^{NHK}, FLAG-tagged malectin, and β-actin were analyzed by immunoblot using the indicated antibodies. (B) Data were quantified as described for Figure 6E. The data shown are mean ± SD from three independent experiments. NS, not significant. (C) HeLa cells were transfected with expression vectors for malectin and FLAG-tagged OS-9 along with expression vectors for AT^{NHK} or AT^{NHK}-Q3. After 24 h, cell lysates were subjected to immunoprecipitation using an anti-FLAG antibody, and then the presence of coimmunoprecipitated AT^{NHK} or AT^{NHK}-Q3 (right) was analyzed by SDS–PAGE under nonreducing conditions. Protein expression was monitored using an anti–human AT antibody, anti–human malectin antibody, or anti-FLAG antibody (left).

single point mutation (Y104A, Y131A, or F132A) or double mutation (Y104A/Y131A, Y104A/F132A, Y104A/D201A, or Y131A/F132A) was overexpressed instead of wild-type malectin (Figure 6, D and E, and Supplemental Figure S5, C and D). Taken together with the data suggesting that folding-deficient AT^{NHK} is recognized by malectin in a sugar-dependent manner (Figure 4B), these results indicated that malectin prevents the secretion of AT^{NHK} through retention of the misfolded glycoprotein in the ER mediated by binding to G2M9 glycan.

Decreased secretion of AT^{NHK} by malectin overexpression is due to enhancement of ERAD

The previous results indicated that AT^{NHK} is retained in the ER by malectin. However, the level of intracellular AT^{NHK} was not increased in malectin-overexpressing cells, despite the fact that secretion of AT^{NHK} was essentially blocked (Figure 6C). Because most newly synthesized AT^{NHK} is degraded through the ERAD pathway, we examined the effect of treatment with the proteasome inhibitor MG132 on the secretion of AT^{NHK} in the presence of malectin overexpression. MG132 strongly inhibits the ERAD pathway by blocking proteasome degradation (Lee and Goldberg, 1998). MG132 treatment resulted in a 1.5-fold increase in the secretion of AT^{NHK} dimers (Figure 7, A and B). By contrast, malectin overexpression did not affect AT^{NHK} secretion in the presence of MG132 (Figure 7, A and B). Overexpression of malectin decreased the secretion of AT^{NHK} in untreated cells, whereas it had no effect on the secretion of AT^{NHK} in MG132-treated cells, indicating that malectin may guide misfolded AT^{NHK} into the proteasome-mediated degradation pathway. To test this, we examined the association of AT^{NHK} with OS-9, a molecular guide for misfolded proteins processed by ERAD. Because OS-9 could trap the ERAD substrates and form a complex with ER membrane-embedded Hrd1-SEL1L ubiquitin ligase, misfolded glycoproteins are retrogradely translocated to the cytosol and degraded by proteasome (Christianson *et al.*, 2008). AT^{NHK} and AT^{NHK}-Q3, but not wild-type AT, interacted with OS-9 (Bernasconi *et al.*, 2008; Hosokawa *et al.*, 2009; Satoh *et al.*, 2010). We coexpressed FLAG-tagged OS-9, malectin, and AT^{NHK} in HeLa cells and confirmed that malectin expression was increased and AT^{NHK} secretion abolished in the transfected cells (unpublished data). The amount of AT^{NHK} that coprecipitated with FLAG-tagged OS-9 was increased by malectin overexpression, whereas there were no significant differences in the amount of AT^{NHK}-Q3 associated with OS-9 (Figure 7C). Based on the sugar-binding specificity of malectin and OS-9 (Hosokawa *et al.*, 2009; Mikami *et al.*, 2010), these results indicated that malectin traps misfolded N-glycosylated proteins and guides them into the ERAD pathway via OS-9 in a sugar-dependent manner. Of interest, malectin mRNA levels were significantly elevated after 12-h treatment of the cells with tunicamycin, an ER-stress inducer, and expression increased in a time-dependent manner over a period of 24 h (Supplemental Figure S3). These data suggest that malectin might function as an ER chaperone to eliminate misfolded substrate, thereby assisting in the quality control of newly synthesized glycoproteins.

DISCUSSION

Previously, we analyzed the sugar-binding capacity and specificity of the intracellular lectins VIP36 (Kawasaki *et al.*, 2007), ERGIC-53 (Kawasaki *et al.*, 2008), VIPL (Yamaguchi *et al.*, 2007), OS-9 (Mikami *et al.*, 2010), XTP3-B (Yamaguchi *et al.*, 2010), and α-glucosidase IIβ (Hu *et al.*, 2009) using FAC and flow cytometry with a lectin tetramer and membrane-based carbohydrates. Although lectin–sugar interactions are weak (K_a ~10^4 M^{-1}), these methods precisely identified native sugar ligands, opening the door to further investigation of the role of these lectins in glycoprotein quality control (Yamamoto and Kawasaki, 2010). Malectin, a type I membrane-anchored ER protein, is an intracellular lectin that was first identified in *X. laevis*. Like other intracellular lectins involved in glycoprotein quality

control, malectin is highly conserved in animals (Schallus *et al.*, 2008). In this study, using a membrane-based assay and FAC, we demonstrated that human malectin binds specifically to G2M9 glycan but not to G1M9 or G3M9. This result was in good agreement with the results of glycan microarray analysis, which showed that malectin selectively binds to Glcα1,3Glc and G2M7GN1 (Schallus *et al.*, 2008; Palma *et al.*, 2010). In the ER, G1M9 glycans expressed on glycoproteins are recognized by the CNX/CRT complex and play an important role in the folding of glycoproteins (Ware *et al.*, 1995). M8B glycan produced by ER α-mannosidase I preferentially binds to the cargo receptor ERGIC-53 for the transport of glycoproteins from the ER to the Golgi (Kawasaki *et al.*, 2008). Trimming of an α1,2-linked mannose from the C-arm of M9 glycan produces M8C, a good ligand of OS-9 and XTP3-B, and results in entry of misfolded glycoproteins into the ERAD pathway, which degrades proteins through an ER membrane–associated ubiquitin ligase (Mikami *et al.*, 2010; Yamaguchi *et al.*, 2010). Until recently, G2M9 glycan was believed to be merely a step in the process of generating G1M9. The demonstration that G2M9 is recognized by the conserved malectin suggests that is has a distinct function, as all of the conserved intracellular lectins appear to participate in glycoprotein quality control by distinguishing N-glycan "tags" on proteins.

Immunoprecipitation analysis of the interaction of malectin with wild-type AT and AT^{NHK} indicated that human malectin selectively binds to misfolded ERAD substrates in a G2M9-dependent manner (Figure 4); by comparison, an association between malectin and wild-type AT was barely detectable. The results of pulse-chase experiments showed that the interaction between AT^{NHK} and malectin is more stable than that between wild-type AT and malectin (Supplemental Figure S2). The mechanism by which malectin distinguishes between misfolded proteins and correctly folded ones has yet to be clarified. One possibility is that malectin and GII coordinately select misfolded proteins at an early stage. Deprez *et al.* (2005) reported that removal of the outermost glucose by GI occurs immediately after N-glycosylation to produce G2M9 glycan. However, efficient trimming of the second glucose from G2M9 by GII only occurs after the second N-glycan is transferred onto the same polypeptide chain. This observation was recently explained by a model in which G2M9 binding to the mannose 6-phosphate receptor homology domain of the GII β-subunit induces a conformational change in the catalytic α-subunit, thus increasing GII activity and allowing the first cleavage to proceed in a nascent G2M9 glycan (Hu *et al.*, 2009; Stigliano *et al.*, 2009). This activation of GII may occur efficiently on correctly folded glycoproteins such as AT. However, in misfolded glycoproteins such as AT^{NHK}, newly transferred N-glycan might be folded irregularly into the peptide and not be easily accessible to GI and GII, resulting in inefficient trimming of another G2M9. The idea that the sugar moieties on AT^{NHK} are inaccessible to sugar-processing enzymes is supported by the observation that the A-arm of N-glycans on AT^{NHK} remains insusceptible to jack bean α-mannosidase treatment (Liu *et al.*, 1999). A second possibility is that malectin itself may act as a folding sensor and trap misfolded glycoproteins or that molecules associated with malectin may recognize misfolded substrates. Barile *et al.* (2005), using coimmunoprecipitation analysis of aquaporin 2, identified a homologue of malectin among other ER-resident molecules such as OST, GI, GII, CNX, and CRT present in immunoprecipitates. A third possibility is that malectin may be part of a folding cycle with UGGT. In the CNX/CRT cycle, UGGT1 functions as a folding sensor by recognizing hydrophobic patches on substrates and transfers a glucose residue to the folding-defective substrates, which causes association between folding-defective proteins and CNX/CRT again (Taylor *et al.*, 2004; Totani *et al.*, 2009). In a similar manner, malectin may bind to misfolded glycoproteins after G1M9 glycans are reglucosylated by an enzyme that also has a folding sensor. UGGT2, a homologue of UGGT1, is one such candidate, although the enzymatic activity, substrate specificity, and intrinsic function of UGGT2 remain unknown (Arnold *et al.*, 2000).

The biological significance of this molecular validation of protein folding by malectin and details of the process were revealed by evaluating the effects of overexpression of malectin on the secretion of AT and AT^{NHK}. The secretion of AT^{NHK} was disrupted by overexpression of malectin via a mechanism that involved N-glycan recognition (Figure 6). In addition, the retardation of AT^{NHK} release from the cell was mostly likely due to ERAD since treatment with MG132 abrogated the decrease in secretion of AT^{NHK} (Figure 7, A and B). In addition, ERAD substrates recognized by OS-9 were significantly elevated (Figure 7C) by overexpression of malectin. The precise mechanism by which malectin guides AT^{NHK} to OS-9 and ultimately to degradation remains to be clarified. EDEM3 is believed to be a key molecule in the degradation of folding-defective glycoproteins (Olivari *et al.*, 2005) since overexpression of EDEM3 enhanced the degradation of AT^{NHK} (Hirao *et al.*, 2006) and EDEM3 and yeast Htm1p possessed α1,2-mannosidase activity and generated OS-9 ligands (Clerc *et al.*, 2009; Hosokawa *et al.*, 2009). Malectin might recruit EDEM3 to induce the ERAD of AT^{NHK}.

The ER is an essential compartment for the synthesis and maturation of membrane-bound and secretory proteins. Perturbation of ER function by inhibition of protein glycosylation or disulfide formation results in the accumulation of misfolded proteins. This leads to ER stress, a state that is defined by the imbalance between the cellular demand for ER function and ER capacity. Under conditions of ER stress, up-regulation of chaperones involved in protein folding and assembly is critical for cell survival (Ni and Lee, 2007). When cells were treated with tunicamycin, an ER-stress inducer, the expression of malectin was significantly enhanced (Supplemental Figure S3). Similar results were demonstrated by thapsigargin treatment (Galli *et al.*, 2011). The obvious augmentation of malectin expression during ER stress implies a unique function for this molecule not only in binding to G2M9 glycans, but also in capturing misfolded glycoproteins and attenuating the cytotoxic effects of their accumulation.

MATERIALS AND METHODS

Cells

HEK293, 293T, and HeLa cells were maintained in DMEM (Invitrogen, Carlsbad, CA) supplemented with 10% heat-inactivated fetal bovine serum (FBS; Invitrogen), 2 mM glutamine, and 25 mM 4-(2-hydroxyethyl)-1-piperazineethanesulfonic acid (HEPES)–NaOH, pH 7.4. HeLaS3 cells were maintained in RPMI 1640 (Invitrogen) supplemented with 10% heat-inactivated FBS and 2 mM glutamine. Cultures were grown at 37°C in a humid atmosphere containing 5% CO_2.

Antibodies

Polyclonal anti-FLAG antibody, monoclonal anti-FLAG antibody (M2), polyclonal anti–human malectin antibody, polyclonal anti–human calnexin antibody, and monoclonal anti–β-actin antibody were purchased from Sigma-Aldrich (St. Louis, MO); polyclonal and monoclonal anti–α1-antitrypsin antibodies were purchased from Abcam (Cambridge, MA).

Reagents

Monosaccharides, including mannose (Man), galactose (Gal), glucose (Glc), L-fucose (Fuc), *N*-acetylglucosamine (GlcNAc),

N-acetylgalactosamine (GalNAc), lactose (Galβ1,4Glc), nigerose (Glcα1,3Glc), and α1,2-mannobiose (Manα1,2Man), were purchased from Wako Pure Chemical Industries (Osaka, Japan). 2-Aminopyridine (PA)-labeled high mannose–type oligosaccharides (G3M9, G2M9, and G1M9) were purchased from Masuda Chemical Industry (Kagawa, Japan).

PCR and nucleotide sequencing

PCR was performed using KOD-plus DNA polymerase (Toyobo, Osaka, Japan). Mutagenesis PCR was performed using Pfu Turbo DNA polymerase (Stratagene, La Jolla, CA). Primers were purchased from Sigma Genosys (Woodlands, TX) or Greiner Bio-One (Solingen, Germany). DNA sequence analysis was done using a Prism 3100 Genetic Analyzer (Applied Biosystems, Foster City, CA).

Construction of *E. coli* expression plasmids for soluble human malectin and malectin mutants

The full-length cDNA of human malectin (NM_014730.2) was amplified by PCR from a cDNA library of human HeLaS3 cells using phosphorylated primers. The sequences of the primers were 5′-CGTGGCGCTGTTTTTCTGAGTCC-3′ and 5′-TTTCTTTCCCACACCCCTCCACC-3′. Amplified products were ligated into the SmaI site of pBluescript II SK(+) to generate pBlue-malectin. With the use of pBlue-malectin as the template, the coding sequence for the soluble luminal domain of malectin (residues 42-228) was amplified by PCR using the primers 5′-GGGAATTCCATATGGCCGGGCTGCCCGAGAGC-3′ and 5′-CGGAATTCCTCCAATCCCGGATGAGGCTG-3′ (*Nde*I and *Eco*RI restriction sites, respectively, are appended). Amplified products were digested with *Nde*I and *Eco*RI and then inserted into the *Nde*I and *Eco*RI sites of pColdI (Takara Bio, Otsu, Japan) to generate pCodI-malectin-Bio. Four malectin mutants, pCodI-malectin(Y104A)-Bio, pCodI-malectin(Y131A)-Bio, pCodI-malectin(F132A)-Bio, and pCodI-malectin(D201A)-Bio, were generated by PCR using pCodI-malectin-Bio as the template and the following primers:

malectin(Y104A)-F, 5′-GTATCAAACTGAGCGGGCCAATGAGGAGACCTTTG-3′;
malectin(Y104A)-R, 5′-CAAAGGTCTCCTCATTGGCCCGCTCAGTTTGATAC-3′;
malectin(Y131A)-F, 5′-GAAATTTGCAGAGGTCGCCTTTGCACAGTCCCAGC-3′;
malectin(Y131A)-R, 5′-GCTGGGACTGTGCAAAGGCGACCTCTGCAAATTTC-3′;
malectin(F132A)-F, 5′-ATTTGCAGAGGTCTACGCTGCACAGTCCCAGCAA-3′;
malectin(F132A)-R, 5′-TTGCTGGGACTGTGCAGCGTAGACCTCTGCAAAT-3′;
malectin(D201A)-F, 5′-GTCAAGGGGTACTATGCCAATCCCAAGGTCTGTG-3′;
and malectin(D201A)-R, 5′-CACAGACCTTGGGATTGGCATAGTACCCCTTGAC-3′.

Construction of mammalian expression plasmids for human malectin and malectin mutants

The cDNA for human malectin lacking its signal sequence was amplified by PCR using pBlue-malectin as the template and the primers 5′- CGGAATTCACCCGGGCTCGGCGTGGCC-3′ and 5′- GCTCTAGATCACAACCGGCAGAGGCAG-3′ (*Eco*RI and *Xba*I sites, respectively, are appended). Amplified products were digested with *Eco*RI and *Xba*I and then inserted into the *Eco*RI and *Xba*I sites of p3xFLAG-CMV9 (Sigma-Aldrich) to generate p3xFLAG-CMV9-malectin. Four malectin mutants, p3xFLAG-CMV9-malectin (Y104A), p3xFLAG-CMV9-malectin (Y131A), p3xFLAG-CMV9-malectin (F132A), and p3xFLAG-CMV9-malectin (D201A), were also generated by PCR using p3xFLAG-CMV9-malectin as the template and the primers described.

Preparation of biotinylated sMAL

BL21(DE3)pLysS *E. coli* transformed with pColdI-malectin-Bio or the mutant derivatives were grown at 37°C in LB media containing 100 μg/ml ampicillin and 25 μg/ml chloramphenicol. When the OD_{600} of the cultures reached 0.5, isopropyl-β-D-thio-galactoside was added to a final concentration of 1 mM, and the cells were kept at 15°C for 30 min. The cultures were incubated for an additional 24 h at 15°C, at which point they were harvested by centrifugation at 5000 × *g* for 15 min at 4°C. The cell pellets were washed with 20 mM phosphate buffer, pH 7.5, containing 150 mM NaCl (PBS) and then resuspended in PBS containing 1 mM phenylmethylsulfonyl fluoride (PMSF) and 10 mM imidazole. The cell suspension was frozen at −80°C and then thawed in cool water. Immediately after the sample was completely thawed, lysozyme (Sigma-Aldrich) was added to a final concentration of 100 μg/ml. Cells were subjected to sonication (level 5; eight times for 20 s each) and then centrifuged at 8000 × *g* for 15 min. The supernatant was collected and applied to a HisTrap HP column (5 ml; GE Healthcare, Uppsala, Sweden) equilibrated with PBS containing 10 mM imidazole. The column was washed with PBS containing 10 mM imidazole and then eluted with a linear gradient of imidazole from 10 to 500 mM in PBS (25 ml total). Elution was performed at a rate of 1 ml/min, and fractions of 1.0 ml were collected. Fractions containing sMAL were identified by SDS–PAGE and pooled. Purified malectin was biotinylated as described previously (Kawasaki *et al.*, 2007). CD spectra of recombinant sMAL were obtained using a Jasco J-725 sepectropolarimeter (Jasco, Tokyo, Japan) at room temperature. Samples contained 0.1–0.2 mg/ml of protein dissolved in 50 mM sodium phosphate buffer, pH 7.4. Each spectrum was recorded as the average of 20 scans over a range of 190–250 nm.

Binding assay

To modify cell surface N-glycans, HeLaS3 cells were treated with the α-glucosidase inhibitor CST (1 mM; Wako) or DNJ (1 mM; Wako) or with the α-mannosidase inhibitor KIF (8.6 μM; Calbiochem, Darmstadt, Germany) or SW (58 μM; Calbiochem) for 20 h before analysis. Treated cells were harvested and then suspended in HEPES-buffered saline (HBS; 20 mM HEPES-NaOH, pH 7.4, 136 mM NaCl, 4.7 mM KCl, 0.2% BSA, 1 mM $CaCl_2$, and 0.1% NaN_3) at a concentration of 2×10^7 cells/ml. An aliquot of the cell suspension (10 μl) was incubated with 10 μl of sMAL complexed with PE-labeled streptavidin (sMAL-SA) at the indicated concentrations at room temperature for 30 min. After washing with HBS, cells were resuspended in 200 μl of HBS containing 0.5% paraformaldehyde and then analyzed by flow cytometry using a FACScalibur system equipped with CELLQuest software (BD Biosciences, San Jose, CA). Mean fluorescence intensity was used as a measure of binding of PE-labeled sMAL-SA to HeLaS3 cells. For monosaccharide and disaccharide inhibition assays, various sugars (Wako) were added to the cells during incubation with PE-labeled sMAL-SA.

Frontal affinity chromatography

Biotinylated human recombinant sMAL was coupled to streptavidin Sepharose (GE Healthcare, Buckinghamshire, United Kingdom) at concentrations of 1.0 and 0.2 mg/ml gel according to the manufacturer's protocol. Malectin–Sepharose was suspended in 10 mM

Tris-HCl, pH 7.4, containing 0.15 M NaCl (TBS) and then packed into a miniature column (2 × 10 mm). FAC was performed using an automated FAC system (FAC-1), as described previously (Tateno *et al.*, 2007). Briefly, malectin–Sepharose columns were slotted into a stainless holder and then connected to the FAC-1 machine. Flow rate and column temperature were kept at 0.125 ml/min and 25°C, respectively. After equilibration with TBS, additional volumes (0.5–0.8 ml) of PA-labeled glycan (3.75–7.5 µM) were successively injected into the columns by an autosampling system. Elution of PA-glycan was monitored by fluorescence at an excitation wavelength of 310 nm and an emission wavelength 380 nm. The elution front relative to that of PA-lactose, that is, $V - V_0$, was then determined. Association constants (K_a) were obtained from $V - V_0$ and B_t according to the FAC equation.

Metabolic labeling and immunoprecipitation

A cDNA encoding human AT was amplified by PCR using cDNA from HepG2 cells as a template. The AT variant AT^{NHK} was generated by PCR-based mutagenesis of the AT cDNA using a QuikChange II site-directed mutagenesis kit (Invitrogen). A third cDNA encoding AT^{NHK} in which the three N-glycosylation–site Asn residues were substituted with Gln (AT^{NHK}-Q3) was generated by PCR-based mutagenesis of the AT^{NHK} cDNA. Wild-type and mutant AT cDNAs were ligated into pcDNA3.1 or pCAGGS (Niwa *et al.*, 1991; a kind gift from J. Miyazaki, Osaka University, Osaka, Japan). HeLa cells were cotransfected with p3xFlag-CMV9-malectin and either pcDNA3.1-AT, pcDNA3.1-AT^{NHK}, or pcDNA3.1-AT^{NHK}-Q3 using Lipofectamine 2000 (Invitrogen), according to the manufacturer's protocol. After 24 h, the transfected cells were starved for 1 h by incubation in cysteine- and methionine-free medium and then metabolically labeled with ^{35}S-methionine and ^{35}S-cysteine (EXPRE^{35}S^{35}S, 100 µCi; PerkinElmer, Waltham, MA) for 3 h. For DNJ treatment, cells were cultured in the presence of 1 mM DNJ during the starvation and radiolabeling procedures. Metabolically labeled cells were washed twice in cold PBS containing only 10 mM sodium phosphate (PBS(−)), harvested using a cell scraper, and then lysed in a solution of 50 mM Tris-HCl, pH 7.5, 1% (vol/vol) Triton X-100, 150 mM NaCl, 20 mM iodoacetamide, 1 mM PMSF, and 1 µg/ml leupeptin.

For pulse-chase experiments, cells were metabolically labeled with ^{35}S-methionine and ^{35}S-cysteine for 30 min. Labeled cells were cultured in complete medium for the "chase" part of the procedure, followed by washing in prewarmed PBS(−). After incubation at 37°C for different times, cells were washed with cold PBS(−) twice and then harvested as described.

Anti-FLAG or anti-AT antibodies were coupled to protein G–Sepharose 4 Fast Flow (GE Healthcare) by gentle rotation at 4°C for 1 h. Cell lysates were precleared with protein G–Sepharose 4 Fast Flow (GE Healthcare) beads by gentle rotation at 4°C for 30 min and then subjected to immunoprecipitation with anti-FLAG or anti-AT antibody–coupled beads for 4 h at 4°C with gentle rotation. The beads were washed three times with a solution of Tris-HCl, pH 7.5, 0.1% (vol/vol) Triton X-100, 150 mM NaCl, 1 mM PMSF, and 1 µg/ml leupeptin. The immunoprecipitates were eluted by boiling in buffer containing 100 mM Tris-HCl, pH 6.8, 4% (wt/vol) SDS, 20% (vol/vol) glycerol, and 0.004% (wt/vol) bromophenol blue in preparation for immunoblot analysis. Following separation by SDS–PAGE, AT, AT^{NHK}, and AT^{NHK}-Q3 were quantified on the basis of radioactivity using a BAS 2000 scanner (FujiFilm, Tokyo, Japan).

Real-time PCR

HEK293 cells were treated with 5 µg/ml tunicamycin for 12 or 24 h. Cells were harvested, and total RNA was extracted using an RNeasy Mini Kit (Qiagen, Valencia, CA), according to the manufacturer's instructions. cDNA was generated with a PrimerScript RT reagent kit (Takara Bio) according to the manufacturer's instruction using 0.5 µg of total RNA. Quantitative real-time PCR was performed using a Smart Cycler real-time PCR system (Takara Bio) and SYBR Premix Ex Taq (Takara Bio). The standard curve for each gene was generated using a series of dilutions of cDNA prepared from the control sample. The amplification reaction was performed by two-step PCR as follows: 40 cycles of denaturation at 95°C for 5 s, followed by extension and detection at 60°C for 30 s. The relative RNA abundance of the target gene transcript was normalized against an endogenous gene, hypoxanthine phosphoribosyl transferase (HRPT). The primers for each gene analyzed were as follows:

HPRT-F(RT), 5′-GGCTCCGTTATGGCGACCCG-3′; HPRT-R(RT), 5′-CGAGCAAGACGTTCAGTCCTGTCC-3′; malectin-F(RT), 5′-GCAAGGACCCTTTGGAAGGC-3′; malectin-R(RT), 5′-GCTGGGACTGTGCAAAGTAG-3′.

ACKNOWLEDGMENTS

This study was supported by a grant from the Core Research for Evolutionary Science and Technology of the Japan Science and Technology Agency and by a Grant-in-Aid for Scientific Research to K.Y. (21390173) from the Ministry of Education, Culture, Sports, Science and Technology, Japan.

REFERENCES

Arnold SM, Fessler LI, Fessler JH, Kaufman RJ (2000). Two homologues encoding human UDP-glucose:glycoprotein glucosyltransferase differ in mRNA expression and enzymatic activity. Biochemistry 39, 2149–2163.

Barile M, Pisitkun T, Yu MJ, Chou CL, Verbalis MJ, Shen RF, Knepper MA (2005). Large scale protein identification in intracellular aquaporin-2 vesicles from renal inner medullary collecting duct. Mol Cell Proteomics 4, 1095–1106.

Bernasconi R, Pertel T, Luban J, Molinari M (2008). A dual task for the Xbp1-responsive OS-9 variants in the mammalian endoplasmic reticulum: inhibiting secretion of misfolded protein conformers and enhancing their disposal. J Biol Chem 283, 16446–16454.

Bukau B, Deuerling E, Pfund C, Craig EA (2000). Getting newly synthesized proteins into shape. Cell 101, 119–122.

Christianson JC, Shaler TA, Tyler RE, Kopito RR (2008). OS-9 and GRP94 deliver mutant alpha1-antitrypsin to the Hrd1-SEL1L ubiquitin ligase complex for ERAD. Nat Cell Biol 10, 272–282.

Clerc S, Hirsch C, Oggier DM, Deprez P, Jakob C, Sommer T, Aebi M (2009). Htm1 protein generates the *N*-glycan signal for glycoprotein degradation in the endoplasmic reticulum. J Cell Biol 184, 159–172.

Deprez P, Gautschi M, Helenius A (2005). More than one glycan is needed for ER glucosidase II to allow entry of glycoproteins into the calnexin/calreticulin cycle. Mol Cell 19, 183–195.

Elbein AD, Tropea JE, Mitchell M, Kaushal GP (1990). Kifunensine, a potent inhibitor of the glycoprotein processing mannosidase I. J Biol Chem 265, 15599–15605.

Galli C, Bernasconi R, Solda T, Calanca V, Molinari M (2011). Malectin participates in a backup glycoprotein quality control pathway in the mammalian ER. PLoS One 6, e16304.

Hammond C, Braakman I, Helenius A (1994). Role of *N*-linked oligosaccharide recognition, glucose trimming, and calnexin in glycoprotein folding and quality control. Proc Natl Acad Sci USA 91, 913–917.

Hartl FU (1996). Molecular chaperones in cellular protein folding. Nature 381, 571–579.

Helenius A, Aebi M (2004). Roles of *N*-linked glycans in the endoplasmic reticulum. Annu Rev Biochem 73, 1019–1049.

Hirao K *et al.* (2006). EDEM3, a soluble EDEM homolog, enhances glycoprotein endoplasmic reticulum-associated degradation and mannose trimming. J Biol Chem 281, 9650–9658.

Hosokawa N, Wada I, Hasegawa K, Yorihuzi T, Tremblay LO, Herscovics A, Nagata K (2001). A novel ER α-mannosidase-like protein accelerates ER-associated degradation. EMBO Rep 2, 415–422.

Hosokawa N, Tremblay LO, You Z, Herscovics A, Wada I, Nagata K (2003). Enhancement of endoplasmic reticulum (ER) degradation of misfolded null Hong Kong α1-antitrypsin by human ER mannosidase I. J Biol Chem 278, 26287–26294.

Hosokawa N, Wada I, Natsuka Y, Nagata K (2006). EDEM accelerates ERAD by preventing aberrant dimer formation of misfolded α1-antitrypsin. Genes Cells 11, 465–476.

Hosokawa N, Wada I, Nagasawa K, Moriyama T, Okawa K, Nagata K (2008). Human XTP3-B forms an endoplasmic reticulum quality control scaffold with the HRD1-SEL1L ubiquitin ligase complex and BiP. J Biol Chem 283, 20914–20924.

Hosokawa N, Kamiya Y, Kamiya D, Kato K, Nagata K (2009). Human OS-9, a lectin required for glycoprotein endoplasmic reticulum-associated degradation, recognizes mannose-trimmed *N*-glycans. J Biol Chem 284, 17061–17068.

Hu D *et al.* (2009). Sugar-binding activity of the MRH domain in the ER α-glucosidase II beta subunit is important for efficient glucose trimming. Glycobiology 19, 1127–1135.

Kawasaki N, Matsuo I, Totani K, Nawa D, Suzuki N, Yamaguchi D, Matsumoto N, Ito Y, Yamamoto K (2007). Detection of weak sugar binding activity of VIP36 using VIP36-streptavidin complex and membrane-based sugar chains. J Biochem 141, 221–229.

Kawasaki N, Ichikawa Y, Matsuo I, Totani K, Matsumoto N, Ito Y, Yamamoto K (2008). The sugar-binding ability of ERGIC-53 is enhanced by its interaction with MCFD2. Blood 111, 1972–1979.

Le A, Steiner JL, Ferrell GA, Shaker JC, Sifers RN (1994). Association between calnexin and a secretion-incompetent variant of human α1-antitrypsin. J Biol Chem 269, 7514–7519.

Lederkremer GZ (2009). Glycoprotein folding, quality control and ER-associated degradation. Curr Opin Struct Biol 19, 515–523.

Lee DH, Goldberg AL (1998). Proteasome inhibitors: valuable new tools for cell biologists. Trends Cell Biol 8, 397–403.

Liu Y, Choudhury P, Cabral CM, Sifers RN (1999). Oligosaccharide modification in the early secretory pathway directs the selection of a misfolded glycoprotein for degradation by the proteasome. J Biol Chem 274, 5861–5867.

Maley F, Trimble RB, Tarentino AL, Plummer TH Jr (1989). Characterization of glycoproteins and their associated oligosaccharides through the use of endoglycosidases. Anal Biochem 180, 195–204.

Mikami K *et al.* (2010). The sugar-binding ability of human OS-9 and its involvement in ER-associated degradation. Glycobiology 20, 310–321.

Ni M, Lee AS (2007). ER chaperones in mammalian development and human diseases. FEBS Lett 581, 3641–3651.

Niwa H, Yamamura K, Miyazaki J (1991). Efficient selection for high-expression transfectants with a novel eukaryotic vector. Gene 108, 193–199.

Nyfeler B, Reiterer V, Wendeler MW, Stefan E, Zhang B, Michnick SW, Hauri HP (2008). Identification of ERGIC-53 as an intracellular transport receptor of α1-antitrypsin. J Cell Biol 180, 705–712.

Olivari S, Galli C, Alanen H, Ruddock L, Molinari M (2005). A novel stress-induced EDEM variant regulating endoplasmic reticulum-associated glycoprotein degradation. J Biol Chem 280, 2424–2428.

Ou WJ, Cameron PH, Thomas DY, Bergeron JJ (1993). Association of folding intermediates of glycoproteins with calnexin during protein maturation. Nature 364, 771–776.

Palma AS, Liu Y, Muhle-Goll C, Butters TD, Zhang Y, Childs R, Chai W, Feizi T (2010). Multifaceted approaches including neoglycolipid oligosaccharide microarrays to ligand discovery for malectin. Methods Enzymol 478, 265–286.

Sasak VW, Ordovas JM, Elbein AD, Berninger RW (1985). Castanospermine inhibits glucosidase I and glycoprotein secretion in human hepatoma cells. Biochem J 232, 759–766.

Satoh T, Chen Y, Hu D, Hanashima S, Yamamoto K, Yamaguchi Y (2010). Structural basis for oligosaccharide recognition of misfolded glycoproteins by OS-9 in ER-associated degradation. Mol Cell 40, 905–916.

Saunier B, Kilker RD Jr, Tkacz JS, Quaroni A, Herscovics A (1982). Inhibition of *N*-linked complex oligosaccharide formation by 1-deoxynojirimycin, an inhibitor of processing glucosidases. J Biol Chem 257, 14155–14161.

Schallus T, Feher K, Sternberg U, Rybin V, Muhle-Goll C (2010). Analysis of the specific interactions between the lectin domain of malectin and diglucosides. Glycobiology 20, 1010–1020.

Schallus T *et al.* (2008). Malectin: a novel carbohydrate-binding protein of the endoplasmic reticulum and a candidate player in the early steps of protein *N*-glycosylation. Mol Biol Cell 19, 3404–3414.

Sifers RN, Brashears-Macatee S, Kidd VJ, Muensch H, Woo SL (1988). A frameshift mutation results in a truncated α1-antitrypsin that is retained within the rough endoplasmic reticulum. J Biol Chem 263, 7330–7335.

Stigliano ID, Caramelo JJ, Labriola CA, Parodi AJ, D'Alessio C (2009). Glucosidase II beta subunit modulates *N*-glycan trimming in fission yeasts and mammals. Mol Biol Cell 20, 3974–3984.

Tateno H, Nakamura-Tsuruta S, Hirabayashi J (2007). Frontal affinity chromatography: sugar-protein interactions. Nat Protoc 2, 2529–2537.

Taylor SC, Ferguson AD, Bergeron JJ, Thomas DY (2004). The ER protein folding sensor UDP-glucose glycoprotein-glucosyltransferase modifies substrates distant to local changes in glycoprotein conformation. Nat Struct Mol Biol 11, 128–134.

Totani K, Ihara Y, Tsujimoto T, Matsuo I, Ito Y (2009). The recognition motif of the glycoprotein-folding sensor enzyme UDP-Glc:glycoprotein glucosyltransferase. Biochemistry 48, 2933–2940.

Travis J, Salvesen GS (1983). Human plasma proteinase inhibitors. Annu Rev Biochem 52, 655–709.

Tulsiani DR, Harris TM, Touster O (1982). Swainsonine inhibits the biosynthesis of complex glycoproteins by inhibition of Golgi mannosidase II. J Biol Chem 257, 7936–7939.

Tulsiani DR, Skudlarek MD, Orgebin-Crist MC (1990). Swainsonine induces the production of hybrid glycoproteins and accumulation of oligosaccharides in male reproductive tissues of the rat. Biol Reprod 43, 130–138.

Ware FE, Vassilakos A, Peterson PA, Jackson MR, Lehrman MA, Williams DB (1995). The molecular chaperone calnexin binds $Glc_1Man_9GlcNAc_2$ oligosaccharide as an initial step in recognizing unfolded glycoproteins. J Biol Chem 270, 4697–4704.

Yamaguchi D, Kawasaki N, Matsuo I, Totani K, Tozawa H, Matsumoto N, Ito Y, Yamamoto K (2007). VIPL has sugar-binding activity specific for high-mannose-type *N*-glycans, and glucosylation of the α1,2 mannotriosyl branch blocks its binding. Glycobiology 17, 1061–1069.

Yamaguchi D, Hu D, Matsumoto N, Yamamoto K (2010). Human XTP3-B binds to α1-antitrypsin variant null Hong Kong via the C-terminal MRH domain in a glycan-dependent manner. Glycobiology 20, 348–355.

Yamamoto K, Kawasaki N (2010). Detection of weak-binding sugar activity using membrane-based carbohydrates. Methods Enzymol 478, 233–240.

Zapun A, Darby NJ, Tessier DC, Michalak M, Bergeron JJ, Thomas DY (1998). Enhanced catalysis of ribonuclease B folding by the interaction of calnexin or calreticulin with ERp57. J Biol Chem 273, 6009–6012.